Check for updates

MST literature review prize 2026

I·M3 Institute of Materials, Minerals & Mining

The formation and characteristics of fine granular areas in the VHCF regime – A review

Materials Science and Technology
1–13
© The Author(s) 2026
Article reuse guidelines:
sagepub.com/journals-permissions
DOI: 10.1177/02670836261485832
journals.sagepub.com/home/mst
Sage

Tobias Schäfer[1], Praveen Kumar Velliyangiri[2], Xiao Shen[1], Ulrich Krupp[2] and Wenwen Song[1]

Abstract

While surface failure is one of the dominant mechanisms for components exposed to fatigue loading in the low- and high-cycle fatigue regimes, the very-high-cycle fatigue regime is dominated by subsurface crack initiation, with crack nucleation occurring within the material interior. This subsurface failure is often characterized by a local grain refinement, forming a nano-grained layer in the vicinity of a stress concentrator. These regions are referred to as fine granular areas (FGAs), and it has been shown that their formation is responsible for the majority of fatigue life. The objective of this review is to summarize the current understanding of FGA formation. Several parameters influencing the proposed formation mechanisms are identified and discussed. Furthermore, morphological and mechanistic resemblances to white etching cracks (WECs) are pointed out. Finally, key challenges and opportunities for future research on FGAs are discussed.

Keywords

FGA, VHCF, fatigue life, crack initiation, subsurface, mechanism, bearing, influencing parameters

Received: 26 June 2026; accepted: 23 August 2026

Introduction

A comprehensive understanding of fatigue behavior of bearing steels is essential for the design and construction of safety-relevant components, as these materials are typically exposed to cyclic loading.[1] Such highly stressed components are present in many industrial sectors, including transportation, energy and construction.[2] They are frequently subjected to low stress amplitudes for extended periods of time and, in most cases surpass 10^7 cycles, placing them within the traditional fatigue limit regime.[3] However, since the late 1990s, it has been well established that material failure can also occur at stress levels significantly below a conventionally defined fatigue limit.[4] This condition, referred to as Very High Cycle Fatigue (VHCF), must therefore be considered in the design of bearing components to prevent premature failures with potentially catastrophic consequences like danger to human life.[3,5] Premature bearing failure, e.g., in wind turbines, also represent a major problem from a sustainable perspective. Replacement of failed bearings in such large-scale systems is an extremely resource- and time-intensive process, related to unexpected downtime, labor-intensive maintenance and increased carbon emissions.[6,7] Moreover, the downtime challenges the sustainability goals of the green transition due to the reduced energy output.

As opposed to a lower number of cycles to failure, where the crack initiates at the component surface, cracks in the VHCF regime typically originate from subsurface defects, such as pores and non-metallic inclusions (NMIs). This phenomenon was first systematically documented in the late 1990s, primarily through pioneering work by renowned research groups from Japan.[8–12] It was found that this damage mechanism is accompanied by a microstructural alteration, resulting in a fine granular area (FGA) in the immediate vicinity of the defect.[12] Various mechanisms have been proposed for the FGA formation, the crack initiation from subsurface defects and the subsequent crack propagation.[9,13–17] According to the investigations, a range of influencing factors, including inclusion characteristics, mechanical loading parameters as well as environmental conditions, play crucial roles in the evolution of FGAs. A thorough understanding of these factors is essential in order to make adequate service life predictions and to enable the design of components with reduced risk of premature failure.

This review presents the postulated mechanisms and discusses various parameters affecting the FGA formation and subsurface crack initiation. To establish the necessary background, the review first outlines historical overview of fatigue testing and the characteristics of VHCF. Furthermore, potential research gaps are identified, as this damage mechanism has not yet been conclusively clarified.

[1]Institute of Materials Engineering, University of Kassel, Kassel, Germany
[2]Steel Institute, RWTH Aachen University, Aachen, Germany

Corresponding author:
Tobias Schäfer, Institute of Materials Engineering, University of Kassel, Mönchebergstr. 7, 34125 Kassel, Germany.
Email: tobias.schaefer@uni-kassel.de

VHCF and fracture behaviors

Definition of VHCF. August Wöhler, one of the pioneers in the field of fatigue testing of metallic samples and components, was the first to systematically investigate fatigue properties in 1870.[18] He discovered that material failure under cyclic loading can occur even if the applied stress is significantly below the tensile strength. The graphical representation of the test results for samples of the same material and geometry is known as the Wöhler curve (S-N curve; S: Stress amplitude, N: Number of cycles to failure). Depending on the applied stress and the corresponding fatigue life, it can typically be divided into three distinct regions: LCF, HCF and VHCF.

The regime of high stress amplitudes and low numbers of cycles to failure, up to approx. 10^4 cycles, is known as Low-Cycle Fatigue (LCF),[19] where the accumulation of plastic strain leads to rapid failure of the material. This relationship is described mathematically by the Coffin-Manson equation.[20] For the range between approx. 10^4 and 10^6 or 10^7 cycles, Basquin demonstrated that there is an exponential relationship between the stress amplitude and the fatigue life, which can be approximated by a straight line in double-logarithmic scale.[21] Beyond this range, which is referred to as High-Cycle Fatigue (HCF),[20] only little experimental data was available for a long period of time due to the long test durations. Depending on the alloy condition, a distinction between two types of material behavior was made.[22] For body-centered cubic (bcc) materials in particular, it was assumed that a defined fatigue limit exists, resulting in a horizontal asymptote in the S-N curve (type I). In contrast, the S-N curve for face-centered cubic (fcc) and hexagonal close-packed (hcp) materials tended to decline further with a reduced slope (type II).

In the late 1970s, the first fatigue tests of metallic samples in regions of much higher load cycles became feasible due to technological advancements and the use of high-frequency testing machines. Concepts of new types of ultrasonic fatigue testing machines operating at a frequency of 20 kHz were published, enabling fatigue tests up to 10^{10} load cycles with relatively short test durations.[23,24] By exploring this new load cycle regime, it was possible to reveal that, contrary to the conventional assumptions of a defined fatigue limit, the regime of Very-High-Cycle Fatigue (VHCF) exists and that material failure can occur even beyond 10^9 cycles.[25] There is no uniform terminology for this fatigue range in the literature, so that other terms such as gigacycle fatigue,[9] ultrahigh-cycle fatigue[26] or ultra-long life fatigue[27] can also be found.

Fracture behavior and fracture surface morphology in VHCF

Generally, the fracture behavior of metallic materials under fatigue loading can be divided into two cases: surface or subsurface crack initiation. The LCF regime is characterized by cracks initiating at the surface and propagating through the interior. In contrast, subsurface crack initiation is mainly found in the VHCF regime. To some extent, subsurface crack initiation can also occur in the HCF regime for materials of higher defect density, like high pore volume due to keyholes or lack of fusion in additive manufacturing processes.[28,29]

Murakami et al.[9] and Nishijima et al.[10] proposed two schematic S-N-curves enhanced for the VHCF regime in 1999. Deviating from earlier assumptions, both show that internal failure occurs in VHCF regime below the conventional fatigue limit. However, according to Mughrabi,[26] the type of failure is not only dependent on the number of loading cycles, but also on the intrinsic material properties, hence he classifies into two distinctive types of materials. His considerations assume that surface crack initiation in the VHCF is only found in ductile, defect-free materials (type I) while subsurface failure is exclusive to materials with internal defects (type II).

A parameter to describe the crack propagation for both surface and subsurface crack initiation is the cyclic stress intensity factor (SIF) from linear elastic fracture mechanics (LEFM). It quantifies the stress concentration within the plastic zone in front of the crack tip.[30] For its calculation, Irwin.[31] introduced an approach, that was later applied in a simplified way to fatigue failure of high strength steels with internal failure by Murakami et al.[32,33] Considering the stress range $\Delta\sigma$ and the projected cross-sectional area $\sqrt{area}$ of a crack-initiating defect perpendicular to the direction of loading, equation 2.1 is obtained. When exceeding the threshold value for cyclic crack propagation ΔK_{th} (4–6 MPa·m$^{1/2}$ for high-strength steels[8]), growth of long fatigue cracks becomes feasible.

$$\Delta K = 0.5 \cdot \Delta\sigma\sqrt{\pi\sqrt{area}} \tag{2.1}$$

Subsurface crack initiation results in a characteristic fracture surface morphology that differs significantly from surface crack initiation. Within the fracture surface, a unique feature can be observed which is called "fish-eye" due to its visual appearance, see Figure 1 a). Decisive parameters and regions of the fish-eye are shown in Figure 1 b). The crack-initiating defect, often an NMI, is located at the center with the crack initiation depth d_{NMI} as its distance to the sample surface. A rough, fine granular area (FGA) forms in the immediate vicinity, which will be examined in detail in the subsequent chapter. In contrast, the outer region of the fish-eye is typically smooth or marked by radial ridges. As this phenomenon occurs preferentially in high strength materials, the final fracture surface is usually characterized by ductile rupture.

Fine granular area

Characteristics of FGA

As mentioned in the previous chapter, an FGA occurs at a subsurface level and can be observed *post mortem* in the fracture surface around the internal defect. Sakai et al. investigated the area in a scanning electron microscope (SEM), and the area appeared to have a fine granular morphology, hence the designation "fine granular area" (FGA).[12] Murakami et al. named it "optically dark area" (ODA), as it appeared as a dark area through the bright-field of a light optical microscope (LOM).[9,35] Other designations are "granular bright facet" (GBF) by Shiozawa et al.,[8] and "rough surface area" (RSA) by Ochi et al..[11]

The FGA plays a crucial role in the failure of metallic materials with subsurface crack origin. Murakami et al. stated

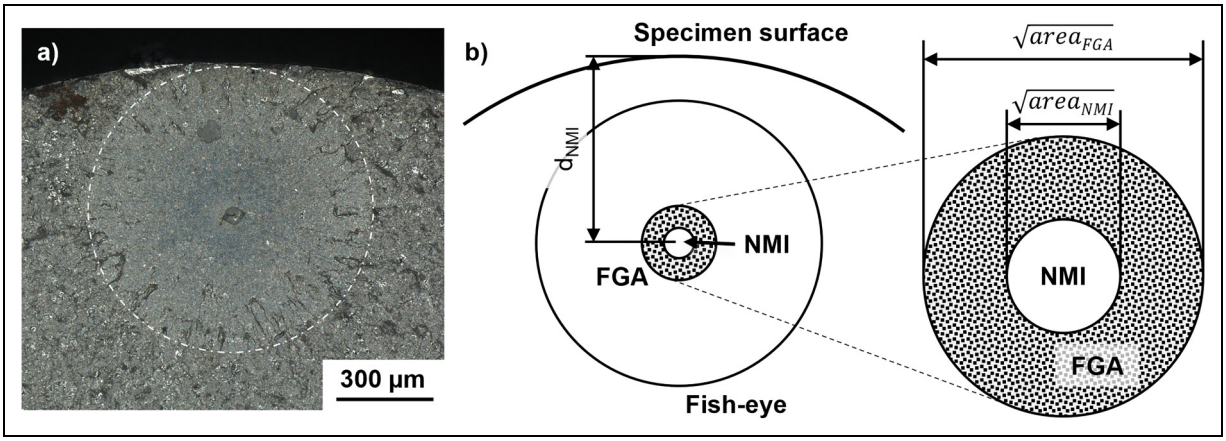


Figure 1. a) Optical micrograph of fish-eye formation in 42CrMo4 steel (fish-eye surrounded by dashed line), b) schematic image of a fish-eye and its parameters. Adapted from.[8,34]

that an increase of the FGA size is associated with an increase of the fatigue life.[35] Investigations by Shiozawa et al. supported this suggestion, as it was shown that a decrease of stress amplitude - and thus extended fatigue life - is accompanied by an increasing FGA size.[27] For further insight into the fracture mechanics, the SIFs both of the NMIs ΔK_{NMI} and the surrounding FGAs (including the inclusion) ΔK_{FGA} were calculated by adjusting Murakami's equation in 2.1. Assuming the compression part of the loading cycle is negligible for crack propagation, the stress range $\Delta\sigma$ was substituted by the stress amplitude σ_a, see equations 3.1 and 3.2. Recently, a software was introduced which enables the automatic calculation of ΔK_{FGA}.[36] By reading in an optical micrograph of a fracture surface, advanced image processing algorithms integrated with a deep learning framework calculate objective and reliable values, which can be an efficient alternative to manual measurement.

$$\Delta K_{NMI} = 0.5 \cdot \sigma_a \sqrt{\pi \sqrt{area_{NMI}}} \tag{3.1}$$

$$\Delta K_{FGA} = 0.5 \cdot \sigma_a \sqrt{\pi \sqrt{area_{FGA}}} \tag{3.2}$$

Equations 3.1 and 3.2 have been proven useful to confirm the significance of the FGA in the VHCF regime regarding the crack propagation. It was found that the SIF at the front of the FGA corresponds to the threshold value ΔK_{th} for stable crack growth[12,27] according to Paris' law.[37] Consequently, the crack growth rate within the FGA happens to be much slower. Hong et al. showed that the crack initiation phase due to the FGA formation accounted for over 95% of the total fatigue life by using Paris equation.[34] By monitoring subsurface cracks in β type Ti-22V-4Al alloy with micro- and nano-scale synchrotron radiation X-ray computed tomography (SR-CT), recent studies by Nakamura and Xue et al.[38,39] have also confirmed that the crack initiation and FGA formation occupy more than 95% of the total fatigue life.

wOver the last decades, several analytical techniques have been conducted to observe the fine granular area and its surroundings in high-strength steels and titanium alloys. Next to the techniques already mentioned, investigations have been done using SEM extended with electron backscatter diffraction (EBSD),[40,41] and transmission Kikuchi diffraction (TKD),[42] transmission electron microscopy (TEM) with selected area diffraction (SAD)[43,44] and atom probe tomography (APT).[45,46] Samples are frequently prepared by employing a focused ion beam (FIB) integrated in an SEM.[47,48]

Microstructural changes and grain refinement within the FGA were observed after VHCF loading in high-strength materials.[15] However, as the FGA is a subsurface phenomenon, its formation and the associated crack evolution remain unresolved. Several mechanisms have been postulated, as outlined below.

Postulated mechanisms of FGA formation

Hydrogen embrittlement. Murakami et al. were the first to postulate a mechanism for the FGA formation and crack initiation inside the fish-eyes.[9] Their investigations of 34CrMo4 and 100Cr6 steels with martensitic microstructure (core hardness values of 500–600 HV) have led to the assumption that the FGA formation is related to hydrogen embrittlement.[9,35,49–51] It is known that hydrogen tends to get trapped at the interface between inclusion and matrix in heat-treated high-strength steels.[52,53] Residual tensile stress, due to a stronger thermal expansion coefficient of the matrix in contrast to the inclusion, superimposed by the applied cyclic stress were also considered to have a detrimental effect on the crack initiation. Under these synergistic conditions, the trapped hydrogen was assumed to enable the initiation of short cracks producing the rough surface around the inclusion, as seen in Figure 2.[9] After reaching a critical threshold value, long crack propagation without the assistance of hydrogen was induced.

By comparing specimens with varying hydrogen contents, Murakami and Nagata have shown that both the fatigue strength and fatigue limit decrease significantly with increasing hydrogen content.[54] Furthermore, in about 70% of hydrogen charged specimens the crack initiating inclusions (aluminum oxides) have been found to be split. Thus, hydrogen was also presumed to be involved in the destruction of inclusions.[54] It is worth noting that an FGA was rarely observed in fracture surfaces of specimens failing in a regime below 10^6 cycles with subsurface crack origin. This emphasizes that not only the trapped hydrogen, but also the repeated cyclic stress in the VHCF regime is responsible for the FGA formation.[54]

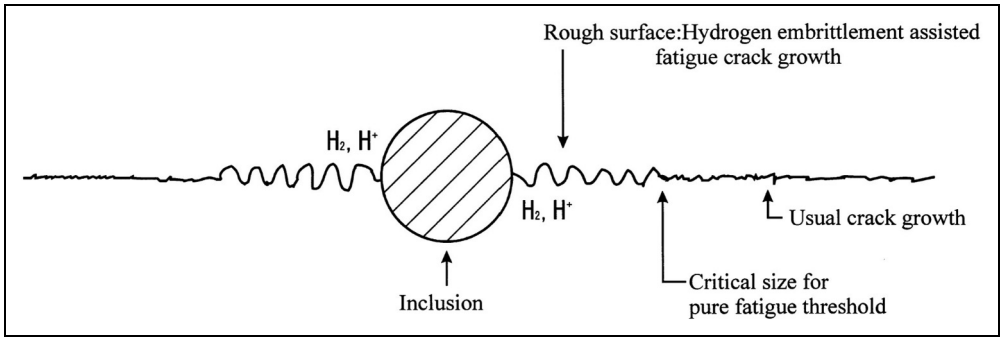


Figure 2. Mechanism schematic by Murakami et al.[9]: Hydrogen embrittlement coupled with cyclic stress. Reprinted with permission from.[9]

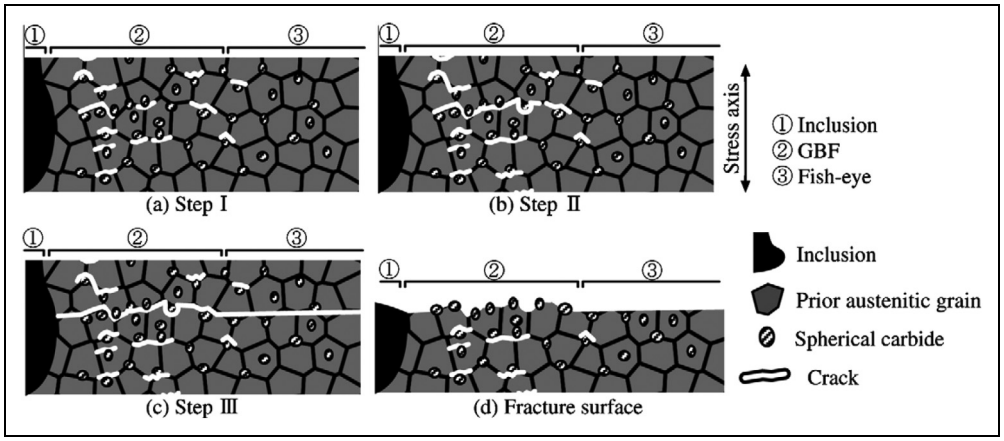


Figure 3. Mechanism schematic by Shiozawa et al.[14]: Dispersive decohesion of spherical carbides. Reprinted with permission from.[14]

Dispersive decohesion of spherical carbides. Shiozawa et al. proposed a formation mechanism related to the decohesion of carbides.[8,14,27] In quenched and tempered steels, iron-carbides are distributed in the matrix due to the heat treatment process.[22,55] Depending on the tempering temperature, the size and volume fraction of the carbides may vary, influencing the resulting hardness values of the material. According to Shiozawa et al., these carbides also play a crucial role in the initiation and propagation of internal cracks.[14] Based on investigations of 100Cr6 bearing steel (hardness values of 750 HV $\pm$ 13.4 HV) by SEM, scanning probe microscopy (SPM) and electron probe microanalysis (EPMA), it was observed that the rough surface within the FGA was due to the decohesion of spherical carbides from the surrounding matrix.

Steps of the proposed mechanism are illustrated in Figure 3.[14] By losing coherence, multiple micro-cracks initiate at the interfaces between carbides and matrix in the vicinity of an NMI (a). Repeating loading cycles then lead to growth and coalescence of the propagating micro-cracks (b). After slowly generating the roughness, the FGA reaches a critical size that enables stable crack propagation regardless of the microstructure, producing the typical fish-eye pattern (c). The surface of the FGA is characterized by remaining carbides or holes, thus its roughness is similar to the size of a spherical carbide (d).

Adhesion and cold-welding. In contrast to the majority of postulated mechanisms, the mechanism proposed by Oguma and Nakamura[16] is not based on experimental research on high-strength steels. Rather than that, the fatigue behavior of duplex (α+β) Ti6Al4 V alloy (hardness value of 316 HV) was investigated by testing compact tension specimens under air and under several different vacuum conditions. For samples tested in high and ultra-high vacuum, granular regions were observed on the fracture surfaces. However, no granular features were confirmed for equal experiments under air or medium vacuum atmosphere. Furthermore, the crack propagation rate was found to decrease with decreasing vacuum pressure. As illustrated in Figure 4,[16] the direct metal-metal contact of crack flanks was assumed to cause a local grain refinement and cold-welding of the crack surfaces during unloading. The path in which the crack propagates in a following loading cycle could differ from the previous one, resulting in fine asperities and roughness on the crack surface.

Furthermore, the mechanism was enhanced by further compression-compression fatigue tests in vacuum.[56] Specimens that consisted of two equal pieces with rounded surfaces touching each other were examined after reaching 10^8 loading cycles. Investigations by SEM, EBSD, TEM and SAD revealed that grain refinement was taking place just beneath the contact surfaces. This indicated that the high number of loading cycles was responsible for the nucleation of dislocations cells and a resulting dynamic recrystallization. Transferring this behavior to subsurface failure in previous experiments, it was assumed that the FGA formation is due to alternating grain refinement and adhesion of the contact surfaces.

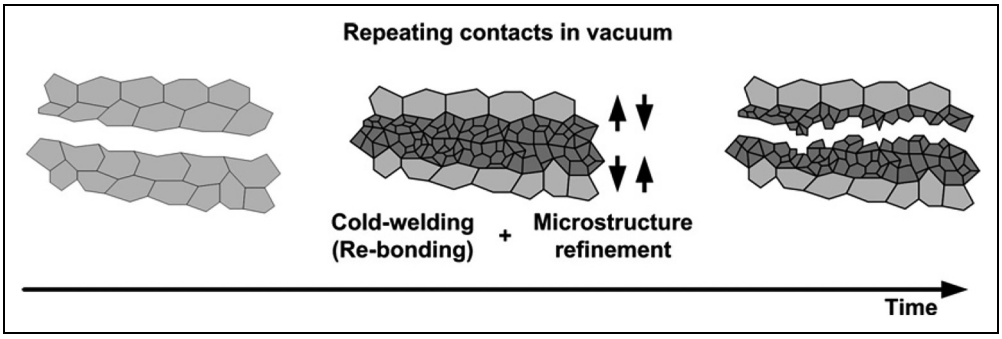


Figure 4. Mechanism schematic by Oguma and Nakamura[16]: adhesion and cold-welding. Reprinted with permission from.[16]

Polygonization. Concluding from investigations of 100Cr6 bearing steel (hardness values of 750–795 HV), the polygonization mechanism was introduced by Sakai et al..[13] In early studies,[12] the different regions of fracture surfaces with internal failure and their corresponding fatigue behavior were classified. Successively, an FGA formed around the inclusion, before cracks propagated stably in the fish-eye region. The remaining fracture surface was assumed to be connected to unstable crack propagation.

The mechanism was specified by conducting scanning ion microscopy (SIM) and SAD of a longitudinal section of the FGA, prepared by FIB.[13] By intensive polygonization around the inclusion due to repeated cyclic loading, a fine granular layer with a thickness of approx. 400 nm happens to form in the first place (a). As a next step, micro-debondings nucleate along the top and bottom boundaries between the fine granular layer and the matrix (b) that eventually coalesce together (c). The adjunction of all the micro-debondings results in a penny-shaped crack and the completion of the rough FGA (d). As the SIF at the front of the FGA ΔK_{FGA} corresponds to the threshold value of stable crack propagation, the aforementioned process was interpreted as the crack initiation phase.[13]

Grain refinement due to dislocations cells. The mechanism proposed by Grad et al.[15] resembles the polygonization model by Sakai et al.,[13] as it is also based on the formation of dislocation cells. The authors questioned if the FGA reaches its final size before cracks start to initiate, or if another chronological sequence should be taken into account. Investigations of fracture surfaces of 100Cr6 bearing steel (hardness value of 780 HV) by SEM revealed that internal failure occurred regardless of the formation of FGAs. For inclusions with SIFs above the threshold value ΔK_{th}, FGAs were not present inside the fish-eyes. Contrary to that, inclusions with lower SIFs were surrounded by FGAs and associated to significantly longer fatigue-life. Cross-sectional samples produced by FIB were analyzed by SIM and TEM with SAD, confirming a local grain refinement around the inclusion.

Figure 5 shows the postulated mechanism,[15] which is explained by changes of the present SIF. As the SIF of the inclusion surpasses the local threshold value, dislocation cells are formed that eventually result in grain refinement in the immediate vicinity of the inclusion (b). Crack initiation becomes feasible by a decreased local threshold value due to the grain refinement (c). Large stress concentrations at the crack tip lead to alternating grain refinement (d) and crack propagation (e), until the SIF of the FGA reaches the global threshold value, enabling stable crack growth and the fish-eye formation (f).

Numerous cyclic pressing. Hong et al.[17] investigated two high-strength steels without standardized designations, however, their chemical compositions closely resemble that of 100Cr6 (hardness values of 753 HV and 760 HV respectively). Samples cut by FIB from regions around crack initiating inclusions were examined by TEM with SAD, confirming the formation of a layer of nanograins on both sides of the fracture surfaces. By experiments under variable stress ratios, it was pointed out that FGA formation only occurred when compressive loading is involved. Based on these results, the mechanism Numerous Cyclic Pressing (NCP) due to repeated crack closure was postulated, as illustrated in Figure 6.[17]

Originating from an inclusion, a fatigue crack initiates due to the cumulative plastic deformation between the inclusion and the matrix caused by cyclic loading (a). The resulting crack wake is then exposed to repeated pressing related to crack closure and the relaxation of residual stress, leading to local grain refinement (b). A nanograin layer is formed due to the interactions between the propagating crack and cyclic pressing of crack surfaces (c). After the FGA reaches a critical size, the transition from slow crack propagation to stable crack growth is marked (d). According to Hong et al.,[17] FGA formation might be considered as a case of severe plastic deformation (SPD), as grain refinement due to applied mechanical load is a characteristic of SPD.[57]

Overview of the postulated mechanisms. An overview of the postulated mechanisms is shown in Table 1, including information on the materials under investigation and their hardness values.

Influencing parameters of FGA formation

Influence of inclusions. As NMIs were involved as local stress concentrators in most of the proposed mechanisms, it is assumed they play a crucial role in the VHCF and in subsurface failure in general. In a review from 2012, it was pointed out that the size, shape, quantity, distribution and composition of NMIs must be taken into consideration regarding the fatigue life in VHCF regime.[58] However, a direct influence on FGA formation was not mentioned. Later that year, a research group around Hong (NCP model) revealed observations on two high carbon chromium steels, one

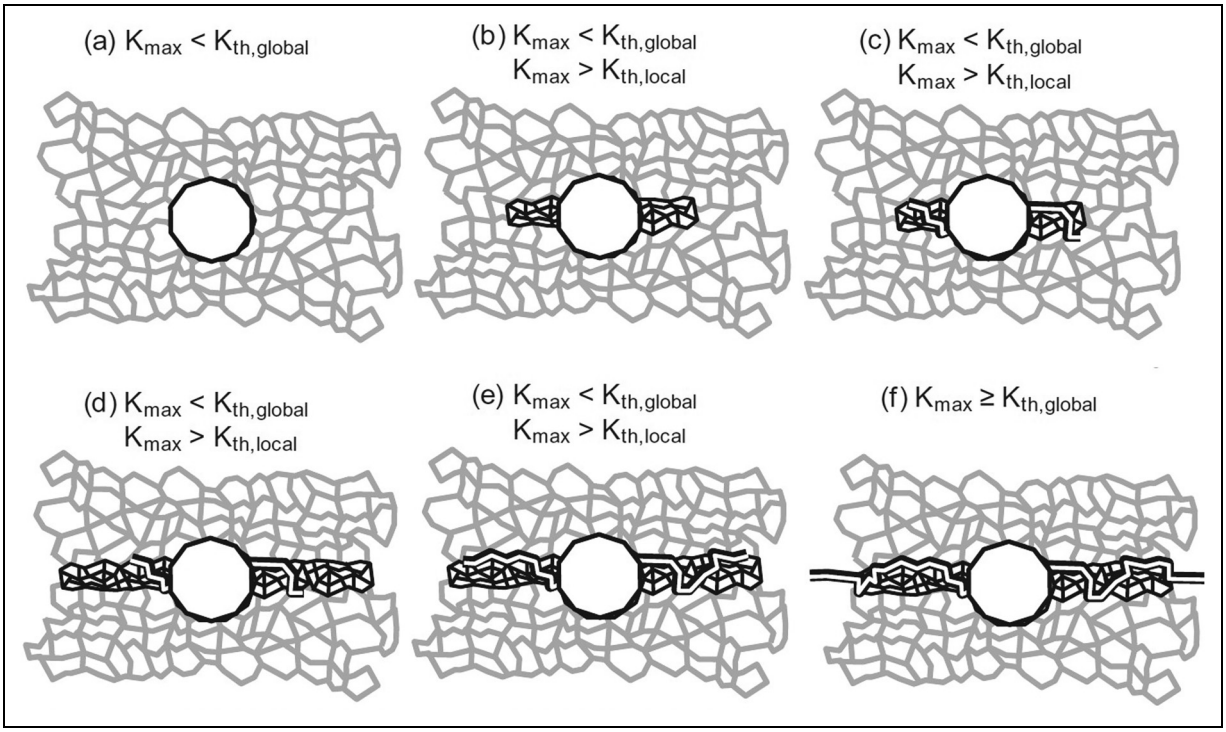


Figure 5. Mechanism schematic by Grad et al.[15]: Grain refinement due to dislocation cells. Reprinted with permission from[15]; compiled by the author.

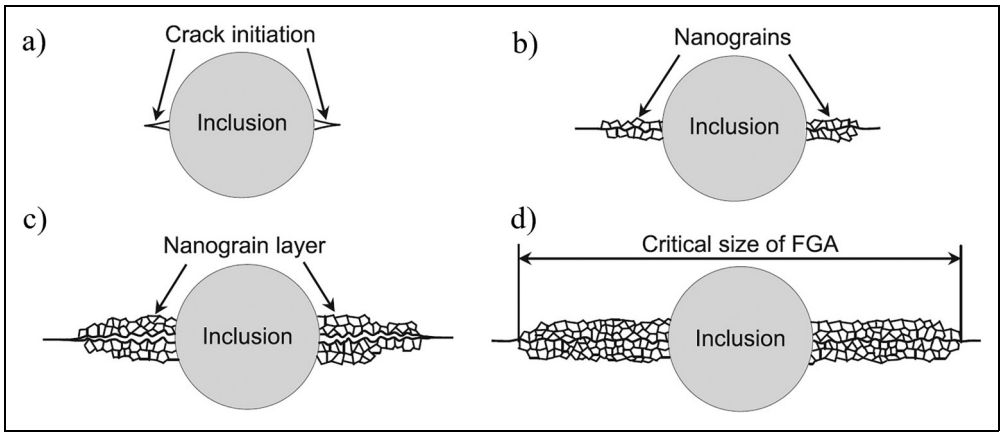


Figure 6. Mechanism schematic by Hong et al.[17]: Numerous Cyclic Pressing (NCP). Reprinted with permission from[17]; compiled by the author.

with small (10–30 μm) and one with large inclusions (20–60 μm).[59] It was shown that the occurrence of an FGA for both uniaxial loading and rotating bending strongly depended on ΔK_{NMI} calculated by equation 3.1. FGA formation became feasible, if the value of ΔK_{NMI} was below the threshold value for stable crack propagation ΔK_{th}. In other words, for large inclusions, FGA formation only occurred in the case of relatively low applied stress amplitudes. Similar results were found for bearing steel 100Cr6.[60,61] Additionally, the inclusion depth d_{NMI} (with respect to the specimen surface) seemed to be an important factor, as an increase in inclusion depth corresponded to a longer fatigue life.

Next to the varying sizes, the chemical composition of the inclusions defines other characteristics like their shape, thermal expansion coefficients, elastic properties and adhesion to the surrounding matrix.[62–66] Fracture surfaces with inclusion-induced internal failure of 100Cr6 were investigated in SEM by Spriesterbach and Grad with special focus on the inclusion type.[67,68] By energy dispersive X-ray spectroscopy (EDX), inclusions were detected to be TiN, CaO, AlCaO and in rare cases MgO type inclusions with respect to the chemical components involved. Measuring their areas showed that the size distribution was much wider for AlCaO and MgO than for CaO and TiN inclusions. These differences also reflect in the values for ΔK_{NMI}, calculated to be in ranges of 3.3–3.68 MPa $m^{1/2}$, 3.29–3.4 MPa $m^{1/2}$, 2.4–2.9 MPa $m^{1/2}$ and 2.09–2.2 MPa $m^{1/2}$, respectively. AlCaO, MgO and some CaO inclusions are known to be heterogeneous, as their chemical components are not evenly distributed. This results in spherical shapes with insufficient bonding properties to the matrix, leading to detachment or decay of

Table 1. Overview of the postulated mechanisms.

Mechanism	Authors	Alloys	Hardness, HV
Hydrogen embrittlement	Murakami et al.[9]	34CrMo4, 100Cr6	500–600
Dispersive decohesion of spherical carbides	Shiozawa et al.[14]	100Cr6	750
Adhesion and cold-welding	Oguma, Nakamura[16,56]	Duplex (α+β) Ti6Al4V	316
Polygonization	Sakai et al.[13]	100Cr6	750–795
Grain refinement due to dislocation cells	Grad et al.[15]	100Cr6	780
Numerous Cyclic Pressing	Hong et al.[17]	Two Steels Similar To 100Cr6	753, 760

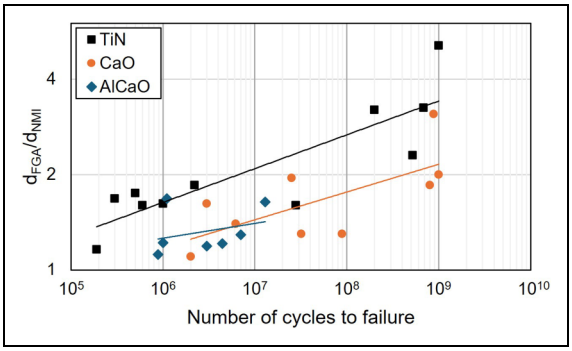


Figure 7. Ratio between FGA and inclusion diameter as a function of the number of cycles to failure. Adapted from.[67]

the inclusions during fatigue loading. Contrary to this, TiN inclusions are homogeneous with even chemical distribution, a sharp-edged cubic morphology and strong coherence to the matrix. They exhibit totally different fracture mechanics, with crack initiation starting in their brittle interior due to the low SIF, leading to an infinite sharp crack able to grow in the matrix.

A direct influence on FGA formation can be seen by comparison of the FGA size relative to the inclusion: Figure 7[67] shows the ratios of mean diameters of FGAs and corresponding inclusions in relation to fatigue life. Considering the same numbers of cycles to failure, TiN inclusions result in larger FGA size compared to AlCaO and CaO.

Influence of load type and loading frequency. Investigations with the scope of comparing the VHCF behavior of 100Cr6 under axial tension-compression loading (AL) and rotating bending (RB) have already been done in the early 2000's.[12,69] It was shown that fatigue strength was significantly higher for RB than for AL under the same material condition. Furthermore, inclusion depth had higher values for AL than for RB in the case of subsurface failure. However, no focus was placed on the direct impact of load type on FGA characteristics.

In later observations, it was demonstrated that FGA size is directly affected by the applied load type.[60,61] Regardless of the type, values of ΔK_{FGA} were in a range between 4–6 MPa·m$^{1/2}$, which is in good relation to the threshold value for stable crack propagation in high-strength steels as already mentioned in chapter 3.1. However, corresponding FGA sizes were much larger for

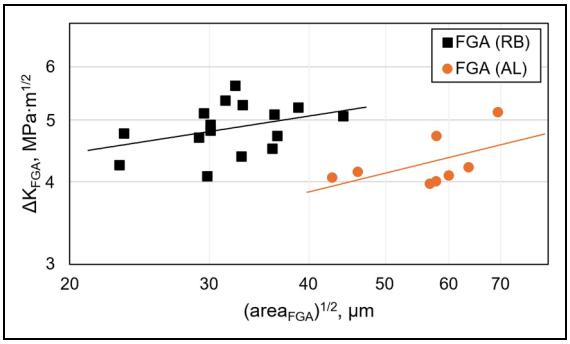


Figure 8. Relationship between ΔK_{FGA} and $\sqrt{area_{FGA}}$ under AL and RB. Adapted from.[60,61]

AL than for RB, as illustrated in Figure 8.[60,61] Similar results were obtained for values of ΔK_{NMI} and inclusion size, which can be explained by different controlling volumes for AL and RB. Considering the same diameter in the specimen's gauge length for both loading types, the highly-stressed volume is reduced to an outer ring for RB due to the stress gradient within the cross-section.[70] This leads to a lower probability for the occurrence of critical inclusions in the controlling volume.

Potential influence of the loading frequency under AL on the VHCF behavior was investigated by Krupp and Giertler for two different steels in two hardness values each.[48,71,72] By comparing resonance fatigue with $f = 95$ Hz and ultrasonic fatigue with $f = 20$ kHz, it was shown that specimens exposed to the higher frequency exhibited higher fatigue strength. It was pointed out that this is primarily attributed to the increased strain rate under ultrasonic loading. At this frequency, a higher applied purely mechanical stress was required to overcome the Peierls stress, mandatory to activate screw dislocation movement.[71] To the best knowledge of the authors, no direct influence of loading frequency on FGA formation has been reported to date.

Influence of mean stress value and stress ratio. The dependence of the FGA formation on stress ratio was already mentioned in chapter 3.2.6 (NCP model).[17] To confirm the validity of the mechanism, ultrasonic axial fatigue tests were examined with stress ratios of $R = -1$, -0.5, 0.1 and 0.3, respectively, by the superposition of conventional tension loading to reach positive mean stress values and increasing stress ratios. By investigating fracture surfaces with internal failure by SEM, TEM and SAD it was shown that FGA occurred regularly for negative stress ratios. While subsurface failure was still dominant for $R = 0.1$, fatigue tests with $R = 0.3$ were mostly accompanied by surface induced failure. For both cases, the shift to positive stress ratios prevented FGA formation.

Conducting comparable fatigue tests with stress ratios of $R = -1$, -0.5, 0.1 and 0.5, Ritz and Beck found similar results for stainless steel X10CrNiMoV12-2-2.[73,74] For $R = -1$ and $R = -0.5$, FGA formation was clearly visible on fracture surfaces. However, the increased mean stress led to a reduced thickness of the refined layer. In the case of $R = 0.1$, FGA formation could partially be observed, while no FGA was found for the highest stress ratio of $R = 0.5$.

Influence of environmental conditions. To investigate the influence of hydrogen on FGA formation, Li et al. examined several

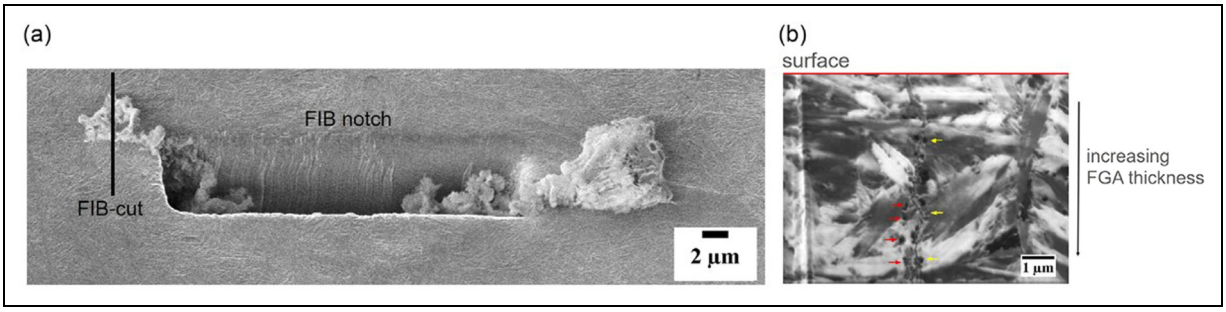


Figure 9. Crack initiation at artificial notch (FIB) after 10^8 cycles at $\sigma_a = 750$ MPa: a) surface cracks at the tips of the notch with pronounced extrusion and b) FIB section showing FGA formation at both sides of the crack flanks (highlighted by the arrows). Giertler and Krupp, *Investigation of Fatigue Damage of Tempered Martensitic Steel during High Cycle Fatigue and Very High Cycle Fatigue Loading Using In Situ Monitoring by Scanning Electron Microscope and High-Resolution Thermography*,[71] licensed under CC BY-NC 4.0.

different high-strength steels in multiple hydrogen pre-charging conditions.[75] In all cases, an increase in hydrogen content reduced the material's fatigue strength significantly. By calculating values of ΔK_{FGA}, a decrease of ΔK_{FGA} was found for pre-charged specimens. It was assumed that internal cracks could therefore propagate under lower stress amplitudes, as ΔK_{FGA} represents the threshold value for stable crack growth. Except for specimens that were charged by soaking instead of cathodic or high-pressure thermal charging, a tendency of increasing FGA size with increasing hydrogen content was also observed. A reduction of ΔK_{FGA} due to hydrogen charging is in good correlation with results by Karsch et al.[76] and Yu et al..[77] However, the tendency of increasing FGA size as a result of increasing hydrogen content is contrary to observations by Yu et al.,[76] as an obvious decrease of FGA size for charged specimens and an accelerated crack growth inside the FGA compared to the uncharged condition was found.

An influence of vacuum atmosphere on FGA formation was already presented in chapter 3.2.3 (adhesion and cold-welding mechanism).[16,56] By conducting compression-compression fatigue tests of two separated rounded samples under vacuum, it was shown that FGA formation can be simulated at specimen surfaces. Spriestersbach et al. performed similar experiments under vacuum to investigate FGA formation in 100Cr6 at artificial surface defects induced by FIB milling in the form of V-notches.[78] To correlate their results with LEFM, SIFs were calculated by considering the size of the defect and the FGA size including the defect size, respectively. As values of ΔK_{FGA} correspond well to the threshold value for stable crack propagation,[12,27] defects with SIFs larger than 4 MPa·m$^{1/2}$ were not surrounded by FGA. All calculated values were in good correlation to internal failure. However, conducting equal experiments in air, no grain refinement was observed around the artificial defect.

Further investigations on artificial defects were conducted by Giertler and Krupp, who integrated an ultrasonic testing device in a SEM.[71] This enabled *in situ* monitoring of the area of interest. Figure 9 a)[71] shows the notch induced by FIB milling and two crack tips after 10^8 loading cycles. The left crack tip in Figure 9 **a)** with pronounced extrusions was then cut by FIB milling to investigate its cross-section. As can be seen in Figure 9 **b)** highlighted by the arrows, a nano-grained layer evolved at both sides of the crack flanks.

Discussions

After several factors have been presented, certain requirements are summarized for the formation of fine granular areas (FGAs) during axial loading (AL) or rotating bending (RB) in the very-high-cycle fatigue (VHCF) regime as below.

FGAs usually occur at a subsurface level originating from internal defects. However, characteristics of FGAs were observed as well at sample surfaces by conducting fatigue tests under vacuum on CT samples,[16] on two-piece samples with a contact surface,[56] and on samples with induced artificial surface defects.[71,78] For equal experiments in air, no grain refinement was found in the vicinity of the crack origin. This indicates that the vacuum-like atmosphere present in sample interior is mandatory to induce FGA formation. Simulating similar conditions by performing fatigue tests inside a vacuum chamber or *in situ* in a scanning electron microscope (SEM) enables possibilities for deeper insights into the underlying complex fracture mechanics.

Furthermore, FGA formation appears to require local stress concentration. In high-strength steels, such stress concentrators are often non-metallic inclusions (NMIs). Spriestersbach and Grad have shown that the elemental components of inclusions define their properties and that some inclusion types are more critical for FGA formation and VHCF failure than others.[67,68] Due to their strong coherence to the matrix, sharp edges and brittle behavior, TiN inclusions have a more detrimental effect than AlCaO inclusions. Contrary to AlCaO inclusions, that decay or detach during fatigue loading, TiN inclusions usually break, representing a harmful sharp crack.[67,79] Under considerations of their respective SIFs, small TiN inclusions enable short crack growth and FGA formation earlier than bigger AlCaO inclusions. Other defects like pores, grain-boundary triple junctions or artificially induced notches in the case of fatigue testing under vacuum have also been proven to act as possible crack origin sites enabling FGA formation.[29,71,78,80] In general, FGA formation occurred if the local SIF of the crack origin site was lower than the global threshold value for long crack propagation of the respective material.

By superimposing ultrasonic AL fatigue with additional tensile test devices, Hong et al.[17] and Ritz and Beck[73,74] revealed that FGA formation is strongly dependent on the applied stress ratio. With decreasing compression loading, FGAs evolved with a reduction in size. For stress ratios of

$R > 0.1$, when no compression loading is involved, FGAs were not found on fracture surfaces. In addition to AL and RB loading, some researchers have also investigated VHCF behavior for torsional loading. Karr et al. conducted ultrasonic torsion fatigue tests of a high-strength spring steel similar to SWOSC-V up to 5×10^9 loading cycles.[81–83] Run-out samples were subsequently tested at an increased stress ratio. Similar to RB, the control volume for torsion loading is reduced due to a stress gradient along the cross-section.[84,85] Moreover, fracture mechanics in torsion loading are dominated by shear stresses, leading to a fracture surface tilted by approx. 45° to the sample's axis. To increase the probability of internal failure, the number and sizes of non-metallic oxide inclusions were intentionally increased by adding iron oxide powder. By comparing varying stress ratios, $R = -1$ was found to be non-detrimental for internal failure, as surface failure was dominant in all cases. Contrary to that, majority of the samples exposed to stress ratios $R = 0.1$ and 0.35 showed internal failure with FGA formation. However, conducting torsion fatigue with $R = -1$ under vacuum, FGA formation was found at surface defects, that were artificially induced by Ar^+ milling. This emphasizes the complexity inherent to this damaging phenomenon.

Several studies have demonstrated that an increasing hardness in quenched and tempered steels leads to a transition of crack initiation sites from surface to subsurface.[48,72,80,86] However, the influence of hardness values and other parameters – such as varying carbon contents and prevailing temperatures – on the formation and characteristics of FGA have not yet been systematically investigated, representing a current gap in knowledge.

To discuss the postulated mechanisms, various influencing parameters on FGA formation should be considered. Mechanisms proposed by Murakami et al.[9] and Shiozawa et al.[14] appear to be valid in the cases of hydrogen-related fatigue failure and decohesion of carbides in steels, respectively. However, because FGA formation was also found in vacuum atmosphere or titanium alloys, hydrogen embrittlement and decohesion of carbides may not be the root causes for subsurface crack initiation and associated grain refinement. Plasticity-driven evolution of dislocation cells around a stress concentrator, leading to grain refinement with low-angle grain boundaries appears to be a plausible explanation. The postulated mechanisms by Sakai et al.,[13] Grad et al.[15] and Hong et al.[17] share similarities regarding the grain refinement. However, the NCP model by Hong et al. appears capable of explaining crack initiation and FGA formation, as it meets the aforementioned requirements: vacuum like atmosphere, a material defect with a SIF $< \Delta K_{th}$, compressive loading involved and a high number of loading cycles. Their approach, that the repeated pressing of crack flanks leads to grain refinement due to crack closure and relaxation effects, gets underlined by the compression-compression tests conducted by Oguma under vacuum.[56] However, the exact time sequence of crack and FGA formation remains debated, as it is unclear whether grain refinement due to localized plasticity is a prerequisite for crack initiation or a consequence of repeated crack closure under compressive loading.

FGAs share similarities with another damaging phenomenon exclusive to components exposed to rolling contact fatigue (RCF).[87] It leads to premature failure of rolling element bearings at 5–10% of the calculated rating life.[88] Investigations of the microstructure by LOM revealed the initiation of subsurface cracks that appear white when treated with a contrast agent, hence the designation white etching crack (WEC).[89] They are usually found around inhomogeneities like NMIs and can branch into a network called white etching area (WEA). As many studies have shown, WECs are as well accompanied by local grain refinement.[89–94] Similar to FGAs, the formation mechanism of WECs is not fully understood, although several mechanisms have been proposed.[95–99] However, only a few studies have been published so far focusing on both FGAs and WECs. Averbeck, Spriestersbach and Kerscher investigated their similarities and expanded the FGA formation mechanism by Grad et al. to WECs,[100,101] showing that both phenomena might have the same root cause.

Conclusions and outlook

The research on FGAs in the VHCF regime plays a pivotal role in understanding fatigue fracture associated with subsurface crack initiation in high-strength materials. As FGA formation strongly influences fatigue life, controlling the mechanism will be essential to meet the requirements in designing modern engineering components. This review has introduced VHCF and its characteristic fracture behavior. Postulated formation mechanisms of the FGA were critically evaluated, and multiple governing parameters were identified. It was revealed that FGA formation is a complex damaging phenomenon, resulting from a highly specific interaction between microstructural properties, and loading as well as environmental conditions.

Key conclusions drawn from this analysis are that FGA formation requires (i) a vacuum-like environment, (ii) local stress concentration within the microstructure and (iii) repeated exposure to mechanical stress. Furthermore, an obvious parallel exists between FGAs and WECs in RCF. Both are related to subsurface cracks, initiating from local stress concentrators like NMIs, and local grain refinement in their vicinity. This suggests that both phenomena could be considered together and that insights from one loading condition (VHCF or RCF) could be used for modeling the other.

For future research on FGAs, key open questions and opportunities emerge:

- A systematic examination of the effects of varying carbon contents, hardness values and testing temperatures may help establish the dependence of FGA formation on these parameters.
- Current studies are largely limited to isolated loading conditions. However, in real-world applications, components are exposed to complex multiaxial loading conditions, such as cyclic axial loading superimposed by alternating torsion.
- A correlation between microstructural features like inclusion characteristics, grain boundaries, dislocation cells and elemental partitioning might extend the current understanding of the FGA formation mechanism. Such a correlation can be realized by investigating a

FIB-cut needle-like specimen in TEM, which is subsequently sharpened for further APT analysis.
- As the FGA formation and associated crack evolution is a subsurface phenomenon, its real-time progression remains invisible to conventional *post mortem* analysis. Conducting ultrasonic fatigue tests on samples with artificially induced surface defects *in situ* in an SEM enables the monitoring of FGA formation and crack propagation.
- Multiscale modeling of inclusions and crack mechanics: Simulating the local stress state due to inclusions with varying properties and crack initiation and propagation might reveal deeper insights into the fracture mechanics and support predicting the onset of failure.

Acknowledgements

The authors would like to express their thanks to the Deutsche Forschungsgemeinschaft (DFG, German Research Foundation) for funding this review in the framework of the project FOR 5701 – White and Dark (project number 523648868).

ORCID iDs

Tobias Schäfer https://orcid.org/0009-0002-7806-4904
Praveen Kumar Velliyangiri https://orcid.org/0000-0002-3626-8346
Xiao Shen https://orcid.org/0000-0002-8946-6821
Ulrich Krupp https://orcid.org/0000-0003-4928-7770
Wenwen Song https://orcid.org/0000-0001-6711-7455

Ethical considerations

There are no human participants in this article and informed consent is not required.

Author contribution(s)

Tobias Schäfer: Conceptualization; Investigation; Visualization; Writing – original draft.
Praveen Kumar Velliyangiri: Writing – review & editing.
Xiao Shen: Writing – review & editing.
Wenwen Song: Conceptualization; Writing – review & editing.
Ulrich Krupp: Writing – review & editing.

Funding

The authors disclosed receipt of the following financial support for the research, authorship, and/or publication of this article: This review was funded by the Deutsche Forschungsgemeinschaft (DFG, German Research Foundation) in the framework of the project FOR 5701 – White and Dark (project number 523648868).

Deutsche Forschungsgemeinschaft, (grant number 523648868).

Declaration of conflicting interests

The authors declared no potential conflicts of interest with respect to the research, authorship, and/or publication of this article.

Data availability statement

The data that support the findings of this study are available from Elsevier but restrictions apply to the availability of these data, which were used under license for the current study, and so are not publicly available. Data are however available from the authors upon reasonable request and with permission of Elsevier.

References

1. Haibach E. *Betriebsfestigkeit: Verfahren und Daten zur Bauteilberechnung*. 3rd ed. Springer-Verlag Berlin Heidelberg, 2006, pp.1–7.
2. Radaj D and Vormwald M. *Ermüdungsfestigkeit: Grundlagen für Ingenieure*. 3rd ed. Springer-Verlag Berlin Heidelberg, 2007, pp.1–5.
3. Läpple V. *Einführung in die Festigkeitslehre*. 4th ed. Springer Fachmedien Wiesbaden, 2016, pp.255–256.
4. Bathias C, Drouillac L and Le Francois P. How and why the fatigue S-N curve does not approach a horizontal asymptote. *Int J Fatigue* 2001; 23: 143–151.
5. Stanzl SE, Tschegg EK and Mayer H. Lifetime measurements for random loading in the very high cycle fatigue range. *Int J Fatigue* 1986; 8: 195–200.
6. De Azevedo M, Araújo AM and Bouchonneau N. A review of wind turbine bearing condition monitoring: state of the art and challenges. *Renewable Sustainable Energy Rev* 2016; 56: 368–379.
7. Su H, Dong L, Yu X, et al. Research on carbon emission for preventive maintenance of wind turbine gearbox based on stochastic differential equation. *Energy Eng* 2024; 121: 973–986.
8. Shiozawa K and Lu L. Very high-cycle fatigue behaviour of shot-peened high-carbon-chromium bearing steel. *Fatigue Fract. Eng. Mater. Struct* 2002; 25: 813–822.
9. Murakami Y, Nomoto T and Ueda T. Factors influencing the mechanism of superlong fatigue failure in steels. *Fatigue Fract. Eng. Mater. Struct* 1999; 22: 581–590.
10. Nishijima S and Kanazawa K. Stepwise S-N curve and fish-eye failure in gigacycle fatigue. *Fatigue Fract. Eng. Mater. Struct* 1999; 22: 601–607.
11. Ochi Y, Matsumura T, Masaki K, et al. High-cycle rotating bending fatigue property in very long-life regime of high-strength steels. *Fatigue Fract. Eng. Mater. Struct* 2002; 25: 823–830.
12. Sakai T, Sato Y and Oguma N. Characteristic S-N properties of high-carbon-chromium-bearing steel under axial loading in long-life fatigue. *Fatigue Fract. Eng. Mater. Struct* 2002; 25: 765–773.
13. Sakai T, Harada H and Oguma N. Crack Initiation Mechanism of Bearing Steel in High Cycle Fatigue. In: Gdoutos EE (ed) Fracture of Nano and Engineering Materials and Structures. *Proceedings of the 16th European Conference of Fracture*, Alexandroupolis, Greece, 3-7 July 2006, pp.1129–1130. Springer Dordrecht.
14. Shiozawa K, et al. Subsurface crack initiation and propagation mechanism in high-strength steel in a very high cycle fatigue regime. *Int J Fatigue* 2006; 28: 1521–1532.
15. Grad P, Reuscher B, Brodyanski A, et al. Mechanism of fatigue crack initiation and propagation in the very high cycle fatigue regime of high-strength steels. *Scr. Mater* 2012; 67: 838–841.
16. Oguma H and Nakamura T. Fatigue crack propagation properties of ti-6Al-4 V in vacuum environments. *Int J Fatigue* 2013; 50: 89–93.
17. Hong Y, Liu X, Lei Z, et al. The formation mechanism of characteristic region at crack initiation for very-high-cycle fatigue of high-strength steels. *Int J Fatigue* 2016; 89: 108–118.

18. Wöhler A. *Ueber die Festigkeits-Versuche mit Eisen und Stahl*. *Zeitschrift für Bauwesen* 1870; 20: 74–106.
19. Coffin LF Jr. Low cycle fatigue-A review. *Appl. Mater. Res* 1962; 1: 129–141.
20. DIN 50100:2022. Schwingfestigkeitsversuch – Durchführung und Auswertung von zyklischen Versuchen mit konstanter Lastamplitude für metallische Werkstoffproben und Bauteile, DIN-Normenausschuss Materialprüfung NMP.
21. Basquin OH. The exponential law of endurance tests. In: ASTM *Proceedings of the thirteenth annual meeting*, Atlantic City, New Jersey, USA, 28 June-2 July 1910, 10: pp.625–630.
22. Macherauch E and Zoch HW. *Praktikum in Werkstoffkunde*. 13th ed. Springer Fachmedien Wiesbaden, 2019, pp.435-439.
23. Stanzl S. A new experimental method for measuring life time and crack growth of materials under multi-stage and random loadings. *Ultrasonics* 1981; 19: 269–272.
24. Weiss B and Stickler R. Ultrasonic fatigue testing of thin-walled stainless steel tubes. *Metall. Trans* 1970; 1: 1057–1060.
25. Bathias C. There is no infinite fatigue life in metallic materials. *Fatigue Fract. Eng. Mater. Struct* 1999; 22: 559–565.
26. Mughrabi H. On 'multi-stage' fatigue life diagrams and the relevant life-controlling mechanisms in ultrahigh-cycle fatigue. *Fatigue Fract. Eng. Mater. Struct* 2002; 25: 755–764.
27. Shiozawa K, Lu L and Ishihara S. S-N curve characteristics and subsurface crack initiation behaviour in ultra-long life fatigue of a high carbon-chromium bearing steel. *Fatigue Fract. Eng. Mater. Struct* 2001; 24: 781–790.
28. Tang D, He X, Wu B, et al. The effect of porosity defects on the mid-cycle fatigue behavior of directed energy deposited ti-6Al-4 V. *Theor. Appl. Fract. Mech* 2022; 119: 103322.
29. Lopes JH, da Costa PR, Freitas M, et al. Review on the fatigue strength of additively manufactured materials under the very high cycle fatigue. *Fatigue Fract. Eng. Mater. Struct* 2025; 48: 979–1000.
30. Richard HA and Sander M. *Ermüdungsrisse*. 2nd ed. Vieweg +Teubner Verlag, 2012, pp.77–82.
31. Irwin GR. Fracture. In: Flügge S (ed) *Fracture, elasticity, plasticity*. Springer Berlin Heidelberg, 1958, pp.551–590.
32. Murakami Y. Analysis of stress intensity factors of modes I, II and III for inclined surface cracks of arbitrary shape. *Eng. Fract. Mech* 1985; 22: 101–114.
33. Murakami Y, Kodama S and Konuma S. Quantitative evaluation of effects of non-metallic inclusions on fatigue strength of high strength steels. I: basic fatigue mechanism and evaluation of correlation between the fatigue fracture stress and the size and location of non-metallic inclusions. *Int J Fatigue* 1989; 11: 291–298.
34. Hong Y, Lei Z, Sun C, et al. Propensities of crack interior initiation and early growth for very-high-cycle fatigue of high strength steels. *Int J Fatigue* 2014; 58: 144–151.
35. Murakami Y, Nomoto T and Ueda T. On the mechanism of fatigue failure in the superlong life regime (N>107 cycles). part 1: influence of hydrogen trapped by inclusions. *Fatigue Fract. Eng. Mater. Struct* 2000; 23: 893–902.
36. Li R, Zhang W, Paolino DS, et al. CALC – ΔK_{th}: atomatic assessment of the stress intensity factor threshold from VHCF fracture surfaces with optically dark area. *Fatigue Fract. Eng. Mater. Struct* 2025; 48: 4071–4803.
37. Paris P and Erdogan F. A critical analysis of crack propagation laws. *J. Basic Eng* 1963; 85: 528–533.
38. Nakamura T, Xue G, Kon Y, et al. Experimental approach for clarifying initiation and growth behaviors of internal fatigue cracks using synchrotron radiation multiscale X-ray computed tomography. *Mater. Perform. Charact* 2023; 12: 107–128.
39. Xue G, Nakamura T, Fujimura N, et al. Full-life growth behavior of a naturally initiated internal fatigue crack in beta titanium alloy via in situ synchrotron radiation multiscale tomography. *Int J Fatigue* 2023; 170: 107571.
40. Sun C, Song Q, Zhou L, et al. The formation of discontinuous gradient regimes during crack initiation in high strength steels under very high cycle fatigue. *Int J Fatigue* 2019; 124: 483–492.
41. Chai G. A study on fatigue damage and crack initiation in austenitic steel matrix during very high cycle fatigue. *Int J Fatigue* 2024; 179: 108033.
42. Zhang HJ, Yu F, Li SX, et al. Fine granular area formation by damage-induced shear strain localization in very-high-cycle fatigue. *Fatigue Fract. Eng. Mater. Struct* 2021; 44: 2489–2502.
43. Tofique MW, Bergström J and Svensson K. Very high cycle fatigue of cold rolled stainless steels, crack initiation and formation of the fine granular area. *Int J Fatigue* 2017; 100: 238–250.
44. Song Q and Sun C. Mechanism of crack initiation and early growth of high strength steels in very high cycle fatigue regime. *Mater. Sci. Eng* 2020; 771: 138648.
45. Spriestersbach D, Grad P, Brodyanski A, et al. Very high cycle fatigue crack initiation: investigation of fatigue mechanisms and threshold values for 100Cr6. In: Christ HJ (ed) *Fatigue of materials at very high numbers of loading cycles*. Springer Fachmedien Wiesbaden, 2018, pp.167–210.
46. Spriestersbach D. *VHCF-Verhalten des hochfesten Stahls 100Cr6: Rissinitiierungsmechanismen und Schwellenwerte*. Dissertation, Technische Universität Kaiserslautern, Germany, 2019.
47. Chai G, Forsman T, Gustavsson F, et al. Formation of fine grained area in martensitic steel during very high cycle fatigue. *Fatigue Fract. Eng. Mater. Struct* 2015; 38: 1315–1323.
48. Krupp U, Koschella K and Giertler A. The significance of grain size, segregations and inclusions for the very high cycle fatigue (VHCF) behavior of tempered martensitic steels. *Procedia Structural Integrity* 2019; 23: 517–522.
49. Murakami Y, Nomoto T and Ueda T. On the mechanism of fatigue failure in the superlong life regime ($N>10^7$ cycles). part II: influence of hydrogen trapped by inclusions. *Fatigue Fract. Eng. Mater. Struct* 2000; 23: 903–910.
50. Murakami Y, Yokoyama NN and Nagata J. Mechanism of fatigue failure in ultralong life regime. *Fatigue Fract. Eng. Mater. Struct* 2000; 25: 735–746.
51. Murakami Y and Yamashita Y. Prediction of life and scatter of fatigue failure originated at nonmetallic inclusions. *Procedia Eng* 2014; 74: 6–11.
52. Hirth JP. Effects of hydrogen on the properties of iron and steel. *Metall Trans A* 1980; 11: 861–890.
53. Takai K, Seki J and Yoshikazu H. Observation of trapping sites of hydrogen and deuterium in high-strength steels by using secondary Ion mass spectrometry. *Mater Trans JIM* 1995; 36: 1134–1139.
54. Murakami Y and Nagata J. Influence factors of fatigue design in ultralong life regime and effect of hydrogen on fatigue

strength of high strength steel. *Trans. Jpn. Spc. Mech. Eng* 2005; 70: 1093–1101.
55. Bargel HJ and Schulze G. *Werkstoffkunde*. 12th ed. Springer Vieweg, 2018, pp.215-218.
56. Oguma H. Formation mechanism of the distinctive granular fracture surface in subsurface fracture of Ti6Al4 V alloy. *Materialia* 2022; 21: 101312.
57. Edalati K, et al. Nanomaterials by severe plastic deformation: review of historical developments and recent advances. *Materials Research Letters* 2022; 10: 163–256.
58. Li SX. Effects of inclusions on very high cycle fatigue properties of high strength steels. *Int. Mater. Rev* 2012; 57: 92–114.
59. Lei Z, Hong Y, Xie J, et al. Effects of inclusion size and location on very-high-cycle fatigue behavior for high strength steels. *Mater. Sci. Eng* 2012; 558: 234–241.
60. Li W, Sakai T, Li Q, et al. Reliability evaluation on very high cycle fatigue property of GCr15 bearing steel. *Int J Fatigue* 2010; 32: 1096–1107.
61. Li W, Sakai T, Li Q, et al. Effect of loading type on fatigue properties of high strength bearing steel in very high cycle regime. *Mater. Sci. Eng* 2011; 528: 5044–5052.
62. Brooksbank D and Andrews KW. Thermal expansion of some inclusions found in steels and relation to tessellated stresses. *J. Iron Steel Inst* 1968; 206: 595–599.
63. Brooksbank D and Andrews KW. Tessellated stresses associated with some inclusions in steels. *J. Iron Steel Inst* 1969; 207: 474–483.
64. Brooksbank D. Thermal expansion of calcium aluminate inclusions and relation to tessellated stresses. *J. Iron Steel Inst* 1970; 208: 495–499.
65. Brooksbank D and Andrews KW. Stress fields around inclusions and their relation to mechanical properties. *J. Iron Steel Inst* 1972; 210: 246–255.
66. Pineau A and Forest S. Effects of inclusions on the very high cycle fatigue behaviour ofsteels. *Fatigue Fract. Eng. Mater. Struct* 2017; 40: 1694–1707.
67. Grad P, Spriestersbach D and Kerscher E. Influence of the inclusion type on the threshold value of failure in the VHCF-regime of high-strength steels. *Adv. Mater. Res* 2014; 891-892: 339–344.
68. Spriestersbach D, Grad P and Kerscher E. Influence of different non-metallic inclusion types on the crack initiation in high-strength steels in the VHCF regime. *Int J Fatigue* 2014; 64: 114–120.
69. Sakai T, et al. Experimental reconfirmation of characteristic S-N property for high carbon chromium bearing steel in wide life region in rotating bending. *J. Soc. Mater. Sci., Jpn.* 2000; 49: 779–785.
70. Nakajima M, Tokaji K, Itoga H, et al. Effect of loading condition on very high cycle fatigue behavior in a high strength steel. *Int J Fatigue* 2010; 32: 475–480.
71. Giertler A and Krupp U. Investigation of fatigue damage of tempered martensitic steel during high cycle fatigue and very high cycle fatigue loading using in situ monitoring by scanning electron microscope and high-resolution thermography. *Steel Res. Int* 2021; 92: 2100268.
72. Krupp U and Giertler A. Surface or internal fatigue crack initiation during VHCF of tempered martensitic and bainitic steels: microstructure and frequency/strain rate dependency. *Metals (Basel)* 2022; 12: 1815.
73. Ritz F and Beck T. Influence of mean stress and notches on the very high cycle fatigue behaviour and crack initiation of a low-pressure steam turbine steel. *Fatigue Fract. Eng. Mater. Struct* 2017; 40: 1762–1771.
74. Ritz F, Stäcker C, Beck T, et al. FGA Formation mechanism for X10CrNiMoV12-2-2 and 34CrNiMo6 for constant and variable amplitude tests under the influence of applied mean loads. *Fatigue Fract. Eng. Mater. Struct* 2018; 41: 1576–1587.
75. Li YD, Chen SM, Liu YB, et al. The characteristics of granular-bright facet in hydrogen pre-charged and uncharged high strength steels in the very high cycle fatigue regime. *J. Mater. Sci* 2010; 45: 831–841.
76. Karsch T, Bomas H, Zoch HW, et al. Influence of hydrogen content and microstructure on the fatigue behaviour of steel SAE 52100 in the VHCF regime. *Int J Fatigue* 2014; 60: 74–89.
77. Yu W, Lv W, He X, et al. Very high cycle fatigue properties of ultrahigh strength steels in the presence of hydrogen. *Mater. Sci. Technol* 2024; 42: 3–10.
78. Spriestersbach D, et al. Very high cycle fatigue of high-strength steels: crack initiation by FGA formation investigated at artificial defects. *Procedia Structural Integrity* 2016; 2: 1101–1108.
79. Monnot J, Heritier R and Cogne JY. Relationship of Melting Practice, Inclusion Type, and Size with Fatigue Resistance of Bearing Steels. In: Hoo JJC (ed) *Effect of Steel Manufacturing Processes on the Quality of Bearing Steels*. ASTM STP 987, 1988, pp.149–165.
80. Krupp U, Solovev M, Honecker F, et al. The potential of self-tempered martensite and bainite in improving the fatigue strength of thermomechanically processed steels. *MATEC Web Conf* 2018; 165: 20006.
81. Karr U, Schönbauer B, Fitzka M, et al. Inclusion initiated fracture under cyclic torsion very high cycle fatigue at different load ratios. *Int J Fatigue* 2019; 122: 199–207.
82. Karr U, Schönbauer BM, Sandaiji Y, et al. Influence of load ratio on torsion very high cycle fatigue of high-strength spring steel in the presence of detrimental defects. *Fatigue Fract. Eng. Mater. Struct* 2021; 44: 2356–2371.
83. Karr U, Schönbauer BM, Sandaiji Y, et al. Effects of non-metallic inclusions and mean stress on axial and torsion very high cycle fatigue of SWOSC-V spring steel. *Metals (Basel)* 2022; 12: 1113.
84. Berns H and Theisen W. *Eisenwerkstoffe – Stahl und Gusseisen.* 4th ed. Springer-Verlag Berlin Heidelberg, 2008, p.79.
85. Hailu YM, et al. The effect of functional gradient material distribution and patterning on torsional properties of lattice structures manufactured using MultiJet fusion technology. *Materials (Basel)* 2021; 14: 6521.
86. Teng X, Pang J, Gao C, et al. Fatigue crack initiation site transition of high-strength steel under very high-cycle fatigue. *Fatigue Fract. Eng. Mater. Struct* 2024; 47: 4450–4464.
87. Bhadeshia HKDH. Steels for bearings. *Prog Mater Sci* 2012; 57: 268–435.
88. Stadler K, Lai J and Vegter RH. A review: the dilemma with premature white etching crack (WEC) bearing failures. In: Beswick JM (ed) *Bearing steel technologies: 10th volume, advances in steel technologies for rolling bearings*. ASTM International, 2014, pp.487–508.
89. Evans MH, Richardson AD, Wang L, et al. Serial sectioning investigation of butterfly and white etching crack (WEC)

formation in wind turbine gearbox bearings. *Wear* 2012; 302: 1573–1582.
90. Averbeck S and Kerscher E. A study of white etching crack formation by compression-torsion experiments. *Frattura ed Integrità Strutturale* 2016; 10: 12–18.
91. Diederichs AM, Schwedt A, Mayer J, et al. Electron microscopy analysis of structural changes within white etching areas. *Mater. Sci. Technol* 2016; 32: 1683–1693.
92. Averbeck S and Kerscher E. Critical plane analysis of multiaxial fatigue experiments leading to white etching crack formation. *J. Phys.: Conf. Ser* 2016; 843: 012028.
93. Danielsen HK, Guzmán FG, Dahl KV, et al. Multiscale characterization of white etching cracks (WEC) in a 100Cr6 bearing from a thrust bearing test rig. *Wear* 2017; 370-371: 73–82.
94. Šmeļova V, Schwedt A, Wang L, et al. Microstructural changes in white etching cracks (WECs) and their relationship with those in dark etching region (DER) and white etching bands (WEBs) due to rolling contact fatigue (RCF). *Int J Fatigue* 2017; 100: 148–158.
95. Evans MH. White structure flaking (WSF) in wind turbine gearbox bearings: effects of 'butterflies' and white etching cracks (WECs). *Mater. Sci. Technol* 2012; 28: 3–22.
96. Ščepanskis M, et al. The numerical model of electrothermal deformations of carbides in bearing steel as the possible cause of white etching cracks initiation. *Tribol. Lett* 2015; 59: 37.
97. Loos J, et al. Influences on generation of white etching crack networks in rolling bearings. *Journal of Mechanics Engineering and Automation* 2016; 6: 85–94.
98. Kadin Y and Sherif MY. Energy dissipation at rubbing crack faces in rolling contact fatigue as the mechanism of white etching area formation. *Int J Fatigue* 2017; 96: 114–126.
99. Manieri F, Stadler K, Morales-Espejel GE, et al. The origins of white etching cracks and their significance to rolling bearing failures. *Int J Fatigue* 2019; 120: 107–133.
100. Averbeck S, Spriestersbach D and Kerscher E. Crack growth and microstructural changes in AISI 52100: white etching cracks (WEC) and fine granular area (FGA). *MATEC Web Conf* 2019; 300: 18001.
101. Averbeck S, Spriestersbach D and Kerscher E. Mechanism of fine granular area and white etching crack formation in AISI 52100 bearing steel. *Theor. Appl. Fract. Mech* 2020; 108: 102664.